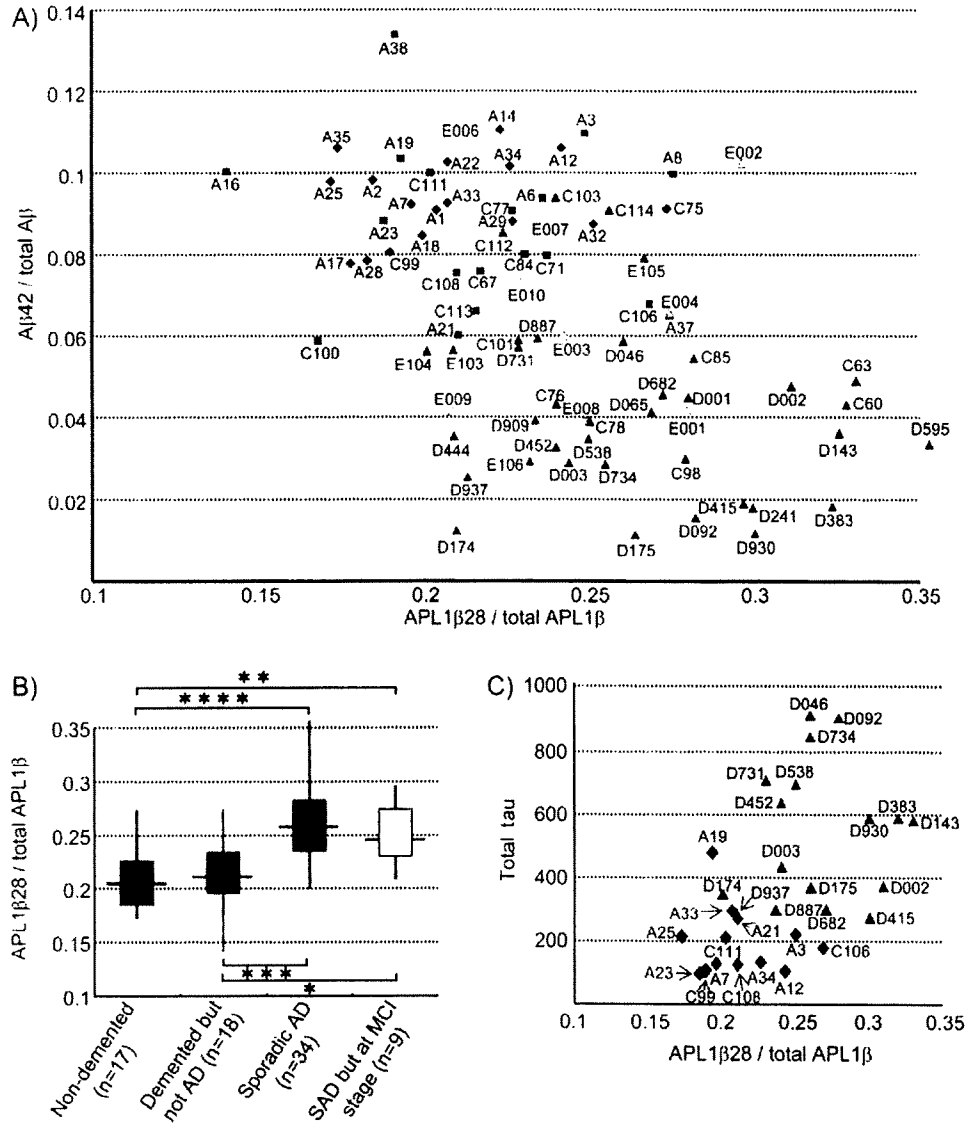

Figure 7. Relative APL1β28 levels in the CSF of sporadic AD and other patients.

A. Relationship between the APL1β28 and the Aβ42 ratio in the CSF. Non-demented, blue rhombus; non-AD, green squares; sporadic AD, red triangles; and sporadic AD at the MCI stage, yellow-filled red triangles.

B. Box plot of the APL1β28 ratio in the CSF of the non-demented, non-AD, sporadic AD and sporadic AD at the MCI stage. Nonparametric statistical analysis was performed (''''$p < 0.0001$, ''' $p < 0.001$, ''$p < 0.01$, '$p < 0.05$).

C. Relationship between the APL1β28 ratio and total tau levels in the CSF. Non-AD, blue rhombus; SAD patients, red triangles.

sporadic AD patients (Andreasen et al, 1999; Jensen et al, 1999; Motter et al, 1995). Finally, the total tau levels, another CSF biomarker of AD, were plotted against the APL1β28 ratios in the CSF of sporadic AD patients and non-demented controls (Fig 7C). Interestingly, the results for sporadic AD patients were located in the upper-right part of the plot. These results indicate that relative APL1β28 levels in CSF are useful for segregating sporadic AD patients. Additionally, no evidence was found for an altered rate of APL1β28 species degradation in CSF (Supplementary Fig 9). Therefore, the relative production of APL1β28 may be up-regulated in the brains of sporadic AD patients.

DISCUSSION

In this study, we identified a novel APLP1-derived peptide species in human CSF. Like AD-associated Aβ, the APL1β are a group of Aβ-like peptides (Okochi et al, 2002) secreted during sequential endoproteolysis by BACE and PS/γ-secretase. Although the APL1β level in CSF is comparable to that of Aβ, we detected the APL1β species in neither senile plaques nor insoluble fractions of AD brain. In cultured cells expressing endogenous wt PS1, some GSMs caused a parallel increase in the relative levels of Aβ42 and APL1β28, the C-terminally elongated

species. Several PS1 FAD mutants also induced such effects. APL1β and Aβ peptide levels were measured in the CSF of patients with PS1 FAD pathological mutations. We found that, although the relative Aβ42 levels in CSF decreased in most of the cases, the relative APL1β28 levels in CSF and the relative APL1β28 generation by mutant-expressing cells increased in parallel. Thus, the results indicate that the level of the novel peptide APL1β28 in CSF is a candidate surrogate marker for brain Aβ42 production.

Disturbances in Aβ42 degradation/clearance are thought to play important roles in the emergence of sporadic AD pathologies (Saido and Iwata, 2006). So far, no study has reported whether there are abnormalities in Aβ42 production in sporadic AD. In this study, we found that APL1β28 and Aβ42 are secreted *in vivo* via similar processes. Thus, we investigated whether the relative level of APL1β28 in the CSF changes in patients with sporadic AD to address whether Aβ42 production changes in the brains of these patients. Strikingly, in sporadic AD, the relative APL1β28 levels in CSF were higher than that of non-AD controls. Moreover, we did not find any evidence for altered degradation of APL1β28 species in the CSF. Collectively, we suggest that (i) relative Aβ42 production in the brain may increase in some sporadic AD patients, as is the case of patients with familial AD, and (ii) that an elevated relative APL1β28 level in the CSF is a potential biomarker for sporadic AD. In the future, we plan to construct an assay system for measuring plasma APL1β and to perform large-scale/cohort studies to determine whether the relative APL1β level in CSF is useful for clinical diagnosis of AD. It will be interesting to determine when the ratio of APL1β28 production starts to rise in the pathological process of sporadic AD.

Using βAPP (Okochi et al, 2006; Weggen et al, 2001), mNotch-1 (Okochi et al, 2006) and APLP1, we found that fenofibrate and S2474 affect the γ-cleavage of multiple substrates. Whether GSMs bind to the TM of APLP1 remains to be determined. If this is the case, although some GSMs may target βAPP (Kukar et al, 2008), their binding would not be specific to βAPP.

Previously, we reported that Nβ, a Notch-1 Aβ-like peptide, is secreted (Okochi et al, 2006), and, in this study, we demonstrated that CSF contains as much APL1β as Aβ. This suggests that a novel group of physiological peptides (*i.e.* a group of Aβ-like peptides) may exist in the human brain. It seems possible that Aβ was identified first because high levels of Aβ accumulation are associated with AD. Because small brain peptides often have a variety of physiological roles, for example serving as neurotransmitters and ligands, it is important to further investigate the physiological functions of Aβ-like peptides such as APL1β and Nβ.

MATERIALS AND METHODS

Antibodies and reagents

Rabbit antisera OA601 and OA663 were raised against the synthetic peptides IQRDELAPAGTGVSRE and DELAPAGTGVSRE, respectively (MBL, Japan). The peptide sequences correspond to the sequence of the human APLP1 juxtamembrane domain (GenBank accession number, U48437). The monoclonal antibody 4G8 against Aβ was purchased from Signet, and the antiserum against APLP1 CTF was purchased from Calbiochem. HRP-conjugated anti-rabbit or anti-mouse IgG (Promega) was used as a secondary antibody. For detection of the biotinylated antibodies, we used neutravidin-HRP (Pierce). The Aβ40 peptide and the peptides DELAPAGTGVSREAVSGLLIMGAGG (APL1β25), DELAPAGTGVSREAVSGLLIMGAGGGS (APL1β27) and DELAPAGTGVSREAVSGLLIMGAGGGSL (APL1β28) were synthesized by Peptide Institute. Each peptide was dissolved in 1,1,1,3,3,3-hexafluoro-2-propanol, stored, and pretreated before use as described previously (Okochi et al, 2006). S2474 was synthesized by Shionogi. The secretase inhibitors L685458 and DAPT were purchased from Peptide Institute, and inhibitor IV and TAPI-1 were from Calbiochem.

Collection of human CSF

Human CSF samples were collected in six facilities. All the experiments using CSF were approved by the ethical committee of Osaka University Hospital (Nos. 07139 and 07212). Lumbar punctures were performed using standard methods. Briefly, CSF (5–10 mL) was collected into sterile polypropylene tubes using atraumatic cannulas (21–23G) placed in the L3/L4 or L4/L5 intervertebral space. CSF was centrifuged for 10 min at 4,000 × *g*, and aliquots of the remaining CSF supernatants were frozen immediately at 80°C. The CSF samples were frozen and thawed once or twice before measurements.

cDNA constructs

A cDNA encoding human APLP1 (Toyobo) was subcloned into pcDNA3.1 Hygro(+). The FAD mutant versions of PS1 were generated by PCR-based mutagenesis using the QuikChange-II kit (Stratagene) with wt PS1 cDNA as a template (Okochi et al, 2002).

Cell culture and cell lines

SH-SY5Y neuroblastoma cells were grown in 1:1 DMEM/F12 media containing 10% fetal calf serum. HEK293 cells stably expressing either wt or mutant PS1, APLP1 and βAPP sw mutant were generated using Lipofectamine 2000 (Invitrogen) and cultured as described previously (Okochi et al, 2000b).

Immunoblotting, combined IP-immunoblotting (IP-blot), and combined IP-autoradiography

For immunoblotting, cell lysates or brain FA-soluble fractions were prepared, diluted in SDS-sample buffer and separated by Tris-glycine or Tris-tricine (Invitrogen) SDS-PAGE as described previously (Okochi et al, 2000b). For analysis of proteins other than APL1β/Aβ, the proteins were transferred to a polyvinylidene difluoride membrane, and for analysis of APL1β/Aβ, the proteins were transferred to a nitrocellulose membrane and boiled for 10 min in phosphate buffered saline (PBS). Membranes were blocked in 5% skim milk and probed with 1:1,000 anti-APLP-1 C-terminal antibody, 1 μg/ml antibody 4G8 or 28 μg/ml biotinylated OA601 IgG, followed by probing with HRP-conjugated anti-rabbit IgG, anti-mouse IgG or neutravidin, respectively. Immunoreactive proteins were detected using ECL or ECL plus reagents (GE Healthcare), and chemiluminescence intensities were measured using a LAS3000 scanner, followed by analysis with Multi Gauge Ver3.0 software (Fuji Film). IP-blot analysis of cultured cell lysates expressing wt APLP1 or mutant PS1 was performed as described previously (Okochi et al, 1997). IP-autoradiography of

The paper explained

PROBLEM:

The 42 amino acid version of amyloid β-peptide (Aβ42) is the major constituent of senile plaques, which is the pathological hallmark of AD and is generated by proteolytic processing of the β-amyloid precursor protein (βAPP). Remarkably, in the CSF of AD patients Aβ42 levels are low, whereas this peptide accumulates within the brain. It is currently believed that this discrepancy may be due to the fact that Aβ42 is largely deposited in insoluble plaques within the brain and that clearance into the CSF is therefore reduced. Although the reverse relationship of Aβ42 levels can be used as a biomarker to some extent after disease onset, better surrogate markers specifically for presymptomatic diagnosis are desperately required.

RESULTS:

In this study, we discovered APL1β28 as a novel and highly sensitive biomarker. This peptide is generated by the same proteolytic mechanism as Aβ42, except that it is derived from a divergent substrate, namely the βAPP-like protein, APLP1. Non-amyloidogenic APL1β28 can be detected in the CSF and its levels correlate with Aβ42 production. Remarkably, the ratio of APL1β28 to total APL1β are significantly increased in familial and sporadic AD cases.

IMPACT:

We propose using the levels of APL1β28 as a surrogate marker for Aβ42 production in the central nervous system. This has clinical importance for the diagnosis and early detection of sporadic AD.

cultured media was performed as described previously (Okochi et al, 2002). Conditioned media collected from radiolabelled SH-SY5Y cells were adjusted to 50 mM Tris (pH 7.4), 1:500 protease inhibitor mix (Sigma) and 5 mM EDTA (pH 8.0) and then immunoprecipitated with OA601.

Combined IP/MALDI-TOF MS (IP/MS) analysis

Combined IP-MALDI-TOF MS analysis was carried out as described previously (Okochi et al, 2002). Either human CSF or conditioned media from SH-SY5Y cells was used. CSF (300 μl) was diluted with 700 μl of Tris buffer (pH 7.6) containing 5 mM EDTA and 1:500 protease inhibitor mix (Sigma). The MS peak heights and molecular masses were normalized to those of angiotensin and bovine insulin β-chain.

Radiolabelled pulse-chase experiment

Following treatments with 1 μM L685458, 10 μM DAPT, or 1 μM inhibitor IV for 16 h, SH-SY5Y cells were metabolically labelled for 8 h as described previously (Okochi et al, 2000a).

Preparation of FA-soluble fractions in human brains

Frozen brains were minced and suspended in two volumes of Tris buffered saline (TBS v/w) supplemented with protease inhibitor mix (Sigma). Suspensions were homogenized with a Teflon homogenizer and centrifuged at 100,000 × *g* for 15 min. The suspensions were extracted twice with 1% Triton X-100 and three times with 2% SDS in TBS, after which the 2% SDS-insoluble fractions were sonicated in FA and then centrifuged at 100,000 × *g* for 15 min. The resultant FA-soluble fractions were evaporated using a Speed-Vac, mixed with 2× SDS-sample buffer and heated for 5 min at 100°C.

Determination of amino acid sequences of APL1β peptides in human CSF

APL1β peptides immunoprecipitated from human CSF by OA601 were eluted with a 20% acetonitrile/0.1% FA solution. The eluates were passed through a 50-kDa filter unit (YM50 Microcon; Millipore), after which the filter was washed twice with the same solution. The resultant filtrates were applied to a C18 column (ODS-100V, TOSOH) using an auto-injection system (Agilent 1100 series). Subsequently, we performed LC/MS/MS analysis using a 50-min gradient (5 to 100% acetonitrile) at a flow rate of 200 μl/min (3200QTRAP; Applied Biosystems). The brain APL1β25, APL1β27 and APL1β28 species were eluted at ~20.7, 21.5 and 22.0 min, respectively. Enhanced mass scan, enhanced resolution and enhanced product ion analyses were performed after elution. All spectra for all peptides in CSF matched those of the synthetic APL1β25, APL1β27 and APL1β28 peptides. Turbo spray was used as an ion source and for each analysis, the curtain gas pressure, collision gas pressure, ion spray voltage, temperature, ion source gas 1 pressure and ion source gas 2 pressure were 15 pounds per squire inch (p.s.i.), 5 p.s.i., 5,500 V, 600°C, 50 and 50 p.s.i., respectively. The declustering potential, enhanced potential and collision cell exit potential were set at 70, 10 and 3 V, respectively. Analyst Version 1.4.1 software was used.

Quantitative LC/MS/MS analysis of APL1β species

Human CSF samples were pretreated using the ProteoSeek™ Albumin/IgG removal kit (PIERCE) according to the manufacturer's instructions. CSF, Cibacron Blue/Protein A gel slurry, and binding/wash buffer were mixed at 2:1:2 (v/v/v) ratio. The pretreated CSF samples were directly applied to a C18 column (ODS-100V; TOSOH) using an auto-injection system (Agilent 1100 series). Conditioned medium was

immunoprecipitated with OA601, and the precipitates were eluted with a solution of 20% acetonitrile and 0.1% FA. The eluates were passed through a 50-kDa filter unit (YM50 Microcon; Millipore). The resultant filtrates were applied to the C18 column. The HPLC parameters were as follows: mobile phase A, 0.1% FA; mobile phase B, acetonitrile with 0.1% FA; mobile phase gradient, 95% A–100% B in 50 min; flow rate, 200 μl/min. After LC/MS/MS analysis (3200QTRAP; Applied Biosystems), the peak areas of the daughter ions (b2, y20 and y21 for APL1β25/28; b2, y21 and y22 for APL1β27) were measured using the Multiquant™ software. The average of three calculated concentrations was defined as the concentration for each APL1β species in the CSF.

Aβ and total tau ELISA

Aβ40 or Aβ42 levels in human CSF or conditioned media were quantified using commercial sandwich ELISA kits (WAKO Pure Chemical Industries, Ltd.). Total tau levels in human CSF were quantified using commercial sandwich ELISA kits (Innogenetics, Belgium). After the addition of the protease inhibitor mixture, human CSF and conditioned media (Sigma) were appropriately diluted with the standard diluents provided in the kits.

In vitro BACE cleavage assay

Recombinant ectodomain BACE1/2 was obtained from R&D Systems, and the synthetic fluorescent peptides wt APP (Nma-EVKM-DAEFK(Dnp)-RR-NH_2) and APLP1 (Nma-EIQR-DELAK(Dnp)-RR-NH_2) were obtained from Peptide Institute Co. Ltd. Recombinant BACE1 or BACE2 (7.4 nM) was mixed with the substrate (1 μM) in the reaction buffer (50 mM sodium acetate, pH 5.0, 0.008% Triton X-100) in a 96-well microtiter plate. The level of fluorescence in each well was determined using a fluorometer (Spectra Max GeminiXS), and the data were analysed using SOFTmax PRO (Molecular Devices).

Fibril formation by APL1β

Fibril formation of Aβ peptide and SEC were previously described (Hartley et al, 1999). Briefly, Aβ1-40, APL1β25, APL1β27 and APL1β28 peptides were dissolved in 1,1,1,3,3,3-hexafluoro-2-propanol to a concentration of 1 mg/ml. Before use, the peptides were dried using a Speed-Vac and dissolved in 1 mM NaOH to a concentration of 1 mM. Solutions were immediately adjusted to pH 7.0 with 10 mM NaOH and diluted to a final concentration of 500 μM in 1:1 water/PBS. Peptides were then incubated at 37°C for 0–48 h and 5-μl aliquots were collected every 4 h. Peptides were diluted with 15 μl of PBS and then centrifuged for 10 min at 16,000 × *g*. Supernatants were fractionated by SEC, and precipitated fibrils were analysed by a transmission electron microscopy (TEM).

SEC

Ten μl of diluted supernatants (protofibrils and low molecular weight peptides) were separated by a Superdex 75 size exclusion column (Hartley et al, 1999) using an AKTA explorer 10S system (GE Healthcare). Peptides were eluted with 50 mM Tris pH 7.6 containing 150 mM NaCl. Elution was monitored by measuring the absorbance at 215 and 280 nm.

TEM

Precipitated fibrils were suspended in 10 μl of PBS. Samples (3 μl) were applied to carbon-coated Maxtaform HF36400 mesh grids (Ohkenshoji) and incubated for 3 min. Excess samples were absorbed with filter paper, after which an equal volume of uranyl acetate solution was added. After incubation for 2 min, the solution was removed and the grid was air-dried. Samples were examined using a Hitachi H-7650 transmission electron microscope.

Immunohistochemistry

Formalin-fixed, paraffin-embedded brain blocks were obtained for immunohistochemistry. Sections (10 μm) cut from these were deparaffinized and pretreated with 0.5% H_2O_2 in PBS for 30 min. The primary antibody was diluted in PBS containing 0.1% Triton X-100 (PBST) and 1% normal serum from the species in which the secondary antibody was raised. After incubation with a specific primary antibody for 48 h at 4°C, the sections were treated with the appropriate biotinylated secondary antibody at 1:1,000 concentration (Vector Laboratories) for 2 h at room temperature. The sections were then washed in PBST and incubated for 2 h at room temperature with avidin-biotinylated HRP complex (ABC Elite; Vector Laboratories). Peroxidase labelling was detected by incubation with a solution containing 0.01% 3,3′-diaminobenzidine (Sigma), 0.6% nickel ammonium sulfate, 0.05 M imidazole and 0.00015% H_2O_2. Negative control experiments were performed as described previously but in the absence of a primary antibody.

Author contributions

KY and MO detected APL1β species in CSF; TSK determined amino acid sequence of APL1β species by LC/MS/MS; ST, TN and TSK measured APL1β by LC/MS/MS; KN, MO and KY performed pulse-chase experiments; MO, JJ and KY performed *in vitro* fibril/protofibril formation assay; KY and ST performed *in vitro* BACE cleavage assay; KY, KN and KM performed Aβ ELISA assay; ST and KY generated PS1 FAD mutant expressing cells; TA performed immunohistochemical study; TI, KK, TT, MK, MI, KD, HK, TT, TM, RH, KT, HA, RK, KT, MT, ST and MO collected CSF samples; HS and CH provided analytical tools and reagents; MO conceived and designed the study, and analysed the data; MO wrote the paper with contributions from HS, CH and ST.

Acknowledgements

We thank Y. Ihara, J. Takeda, A. Carlson, M. Nishimura, H. Hasegawa, K. Horie, C. Kokubu, G. Kondo, Y. Tsujimoto and Y. Eguchi for critical discussions and K. Fujii for technical assistance. MO and coworkers are funded by the National Institute of Biomedical Innovation (05-26), the Ministry of Education, Culture, Sports, Science and Technology, and the Ministry of Health, Labor and Welfare, Japan.

Supplementary information is available at EMBO Molecular Medicine Online.

The authors declare no competing financial interests.

References

Andreasen N, Hesse C, Davidsson P, Minthon L, Wallin A, Winblad B, Vanderstichele H, Vanmechelen E, Blennow K (1999) Cerebrospinal fluid beta-amyloid(1–42) in Alzheimer disease: differences between early- and late-onset Alzheimer disease and stability during the course of disease. Arch Neurol 56: 673-680

Araki Y, Miyagi N, Kato N, Yoshida T, Wada S, Nishimura M, Komano H, Yamamoto T, De Strooper B, Yamamoto K, *et al* (2004) Coordinated metabolism of Alcadein and amyloid beta -protein precursor regulates FE65-dependent gene transactivation. J Biol Chem 279: 24343-24354

Borchelt DR, Thinakaran G, Eckman CB, Lee MK, Davenport F, Ratovitsky T, Prada CM, Kim G, Seekins S, Yager D, *et al* (1996) Familial Alzheimer's disease-linked presenilin 1 variants elevate Abeta1-42/1-40 ratio in vitro and in vivo. Neuron 17: 1005-1013

Citron M, Westaway D, Xia W, Carlson G, Diehl T, Levesque G, Johnson-Wood K, Lee M, Seubert P, Davis A, *et al* (1997) Mutant presenilins of Alzheimer's disease increase production of 42-residue amyloid beta-protein in both transfected cells and transgenic mice. Nat Med 3: 67-72

Coulson EJ, Paliga K, Beyreuther K, Masters CL (2000) What the evolution of the amyloid protein precursor supergene family tells us about its function. Neurochem Int 36: 175-184

De Strooper B (2003) Aph-1, Pen-2, and Nicastrin with Presenilin generate an active gamma-Secretase complex. Neuron 38: 9-12

Edbauer D, Winkler E, Regula JT, Pesold B, Steiner H, Haass C (2003) Reconstitution of gamma-secretase activity. Nat Cell Biol 5: 486-488

Eggert S, Paliga K, Soba P, Evin G, Masters CL, Weidemann A, Beyreuther K (2004) The proteolytic processing of the amyloid precursor protein gene family members APLP-1 and APLP-2 involves alpha-, beta-, gamma-, and epsilon-like cleavages: modulation of APLP-1 processing by n-glycosylation. J Biol Chem 279: 18146-18156

Farzan M, Schnitzler CE, Vasilieva N, Leung D, Choe H (2000) BACE2, a beta -secretase homolog, cleaves at the beta site and within the amyloid-beta region of the amyloid-beta precursor protein. Proc Natl Acad Sci USA 97: 9712-9717

Francis R, McGrath G, Zhang J, Ruddy DA, Sym M, Apfeld J, Nicoll M, Maxwell M, Hai B, Ellis MC, *et al* (2002) aph-1 and pen-2 are required for Notch pathway signaling, gamma-secretase cleavage of betaAPP, and presenilin protein accumulation. Dev Cell 3: 85-97

Fukuyama R, Mizuno T, Mori S, Nakajima K, Fushiki S, Yanagisawa K (2000) Age-dependent change in the levels of Abeta40 and Abeta42 in cerebrospinal fluid from control subjects, and a decrease in the ratio of Abeta42 to Abeta40 level in cerebrospinal fluid from Alzheimer's disease patients. Eur Neurol 43: 155-160

Hartley DM, Walsh DM, Ye CP, Diehl T, Vasquez S, Vassilev PM, Teplow DB, Selkoe DJ (1999) Protofibrillar intermediates of amyloid beta-protein induce acute electrophysiological changes and progressive neurotoxicity in cortical neurons. J Neurosci 19: 8876-8884

Hussain I, Powell D, Howlett DR, Tew DG, Meek TD, Chapman C, Gloger IS, Murphy KE, Southan CD, Ryan DM, *et al* (1999) Identification of a novel aspartic protease (Asp 2) as beta-secretase. Mol Cell Neurosci 14: 419-427

Hussain I, Powell DJ, Howlett DR, Chapman GA, Gilmour L, Murdock PR, Tew DG, Meek TD, Chapman C, Schneider K, *et al* (2000) ASP1 (BACE2) cleaves the amyloid precursor protein at the beta-secretase site. Mol Cell Neurosci 16: 609-619

Ida N, Hartmann T, Pantel J, Schroder J, Zerfass R, Forstl H, Sandbrink R, Masters CL, Beyreuther K (1996) Analysis of heterogeneous A4 peptides in human cerebrospinal fluid and blood by a newly developed sensitive Western blot assay. J Biol Chem 271: 22908-22914

Jensen M, Schroder J, Blomberg M, Engvall B, Pantel J, Ida N, Basun H, Wahlund LO, Werle E, Jauss M, *et al* (1999) Cerebrospinal fluid A beta42 is increased early in sporadic Alzheimer's disease and declines with disease progression. Ann Neurol 45: 504-511

Kauwe JS, Jacquart S, Chakraverty S, Wang J, Mayo K, Fagan AM, Holtzman DM, Morris JC, Goate AM (2007) Extreme cerebrospinal fluid amyloid beta levels identify family with late-onset Alzheimer's disease presenilin 1 mutation. Ann Neurol 61: 446-453

Kimberly WT, LaVoie MJ, Ostaszewski BL, Ye W, Wolfe MS, Selkoe DJ (2003) Gamma-secretase is a membrane protein complex comprised of presenilin, nicastrin, Aph-1, and Pen-2. Proc Natl Acad Sci USA 100: 6382-6387

Kuhn PH, Marjaux E, Imhof A, De Strooper B, Haass C, Lichtenthaler SF (2007) Regulated intramembrane proteolysis of the interleukin-1 receptor II by alpha-, beta-, and gamma-secretase. J Biol Chem 282: 11982-11995

Kukar T, Murphy MP, Eriksen JL, Sagi SA, Weggen S, Smith TE, Ladd T, Khan MA, Kache R, Beard J, *et al* (2005) Diverse compounds mimic Alzheimer disease-causing mutations by augmenting Abeta42 production. Nat Med 11: 545-550

Kukar TL, Ladd TB, Bann MA, Fraering PC, Narlawar R, Maharvi GM, Healy B, Chapman R, Welzel AT, Price RW, *et al* (2008) Substrate-targeting gamma-secretase modulators. Nature 453: 925-929

Lammich S, Okochi M, Takeda M, Kaether C, Capell A, Zimmer AK, Edbauer D, Walter J, Steiner H, Haass C (2002) Presenilin-dependent intramembrane proteolysis of CD44 leads to the liberation of its intracellular domain and the secretion of an Abeta-like peptide. J Biol Chem 277: 44754-44759

Masters CL, Simms G, Weinman NA, Multhaup G, McDonald BL, Beyreuther K (1985) Amyloid plaque core protein in Alzheimer disease and Down syndrome. Proc Natl Acad Sci USA 82: 4245-4249

Mehta PD, Pirttila T, Mehta SP, Sersen EA, Aisen PS, Wisniewski HM (2000) Plasma and cerebrospinal fluid levels of amyloid beta proteins 1–40 and 1–42 in Alzheimer disease. Arch Neurol 57: 100-105

Motter R, Vigo-Pelfrey C, Kholodenko D, Barbour R, Johnson-Wood K, Galasko D, Chang L, Miller B, Clark C, Green R *et al* (1995) Reduction of beta-amyloid peptide42 in the cerebrospinal fluid of patients with Alzheimer's disease. Ann Neurol 38: 643-648

Okochi M, Eimer S, Bottcher A, Baumeister R, Romig H, Walter J, Capell A, Steiner H, Haass C (2000a) A loss of function mutant of the presenilin homologue SEL-12 undergoes aberrant endoproteolysis in Caenorhabditis elegans and increases abeta 42 generation in human cells. J Biol Chem 275: 40925-40932

Okochi M, Fukumori A, Jiang J, Itoh N, Kimura R, Steiner H, Haass C, Tagami S, Takeda M (2006) Secretion of the Notch-1 Abeta-like peptide during Notch signaling. J Biol Chem 281: 7890-7898

Okochi M, Ishii K, Usami M, Sahara N, Kametani F, Tanaka K, Fraser PE, Ikeda M, Saunders AM, Hendriks L, *et al* (1997) Proteolytic processing of presenilin-1 (PS-1) is not associated with Alzheimer's disease with or without PS-1 mutations. FEBS Lett 418: 162-166

Okochi M, Steiner H, Fukumori A, Tanii H, Tomita T, Tanaka T, Iwatsubo T, Kudo T, Takeda M, Haass C (2002) Presenilins mediate a dual intramembranous gamma-secretase cleavage of Notch-1. Embo J 21: 5408-5416

Okochi M, Walter J, Koyama A, Nakajo S, Baba M, Iwatsubo T, Meijer L, Kahle PJ, Haass C (2000b) Constitutive phosphorylation of the Parkinson's disease associated alpha-synuclein. J Biol Chem 275: 390-397

Saido TC, Iwata N (2006) Metabolism of amyloid beta peptide and pathogenesis of Alzheimer's disease. Towards presymptomatic diagnosis, prevention and therapy. Neurosci Res 54: 235-253

Selkoe DJ (2001) Alzheimer's disease: genes, proteins, and therapy. Physiol Rev 81: 741-766

Sinha S, Anderson JP, Barbour R, Basi GS, Caccavello R, Davis D, Doan M, Dovey HF, Frigon N, Hong J, *et al* (1999) Purification and cloning of amyloid precursor protein beta-secretase from human brain. Nature 402: 537-540

Southwick PC, Yamagata SK, Echols CL, Jr. Higson GJ, Neynaber SA, Parson RE, Munroe WA (1996) Assessment of amyloid beta protein in cerebrospinal fluid as an aid in the diagnosis of Alzheimer's disease. J Neurochem 66: 259-265

Takasugi N, Tomita T, Hayashi I, Tsuruoka M, Niimura M, Takahashi Y, Thinakaran G, Iwatsubo T (2003) The role of presenilin cofactors in the gamma-secretase complex. Nature 422: 438-441

Vassar R, Bennett BD, Babu-Khan S, Kahn S, Mendiaz EA, Denis P, Teplow DB, Ross S, Amarante P, Loeloff R, *et al* (1999) Beta-secretase cleavage of Alzheimer's amyloid precursor protein by the transmembrane aspartic protease BACE. Science 286: 735-741

Weggen S, Eriksen JL, Das P, Sagi SA, Wang R, Pietrzik CU, Findlay KA, Smith TE, Murphy MP, Bulter T, *et al* (2001) A subset of NSAIDs lower amyloidogenic Abeta42 independently of cyclooxygenase activity. Nature 414: 212-216

Wiltfang J, Esselmann H, Bibl M, Hull M, Hampel H, Kessler H, Frolich L, Schroder J, Peters O, Jessen F, *et al* (2007) Amyloid beta peptide ratio 42/40 but not A beta 42 correlates with phospho-Tau in patients with low- and high-CSF A beta 40 load. J Neurochem 101: 1053-1059

Wong HK, Sakurai T, Oyama F, Kaneko K, Wada K, Miyazaki H, Kurosawa M, De Strooper B, Saftig P, Nukina N (2005) beta Subunits of voltage-gated sodium channels are novel substrates of beta-site amyloid precursor protein-cleaving enzyme (BACE1) and gamma-secretase. J Biol Chem 280: 23009-23017

Yan R, Bienkowski MJ, Shuck ME, Miao H, Tory MC, Pauley AM, Brashier JR, Stratman NC, Mathews WR, Buhl AE, *et al* (1999) Membrane-anchored aspartyl protease with Alzheimer's disease beta-secretase activity. Nature 402: 533-537

Yu G, Nishimura M, Arawaka S, Levitan D, Zhang L, Tandon A, Song YQ, Rogaeva E, Chen F, Kawarai T, *et al* (2000) Nicastrin modulates presenilin-mediated notch/glp-1 signal transduction and betaAPP processing. Nature 407: 48-54

Acta Neuropathol (2009) 118:647–658
DOI 10.1007/s00401-009-0594-0

ORIGINAL PAPER

Plasma phosphorylated-TDP-43 protein levels correlate with brain pathology in frontotemporal lobar degeneration

Penelope G. Foulds · Yvonne Davidson · Manjari Mishra · David J. Hobson · Kirsty M. Humphreys · Mark Taylor · Nancy Johnson · Sandra Weintraub · Haruhiko Akiyama · Tetsuaki Arai · Masato Hasegawa · Eileen H. Bigio · Fiona E. Benson · David Allsop · David M. A. Mann

Received: 20 February 2009 / Revised: 22 September 2009 / Accepted: 22 September 2009 / Published online: 13 October 2009

Abstract In the present study, we have correlated plasma TDP-43 levels, as measured by ELISA, with the presence of TDP-43 pathological changes in the brains of 28 patients with frontotemporal lobar degeneration (FTLD) (14 with FTLD-TDP and 14 with FTLD-tau) and 24 patients with pathologically confirmed AD (8 with, and 16 without, TDP-43 pathological changes). Western blotting revealed full-length TDP-43, including a phosphorylated form, and a phosphorylated C-terminal fragment, in all samples examined. Both ELISA and immunohistochemistry were performed using phospho-dependent and phospho-independent TDP-43 antibodies for detection of phosphorylated and total TDP-43, respectively. Over all 52 cases, plasma levels of TDP-43, and scores of brain TDP-43 pathology, determined using TDP-43 phospho-dependent antibody correlated with the equivalent measure determined using the TDP phospho-independent antibody. In FTLD, but not AD, TDP-43 plasma levels correlated significantly with the pathology score when using the TDP-43 phospho-dependent antibody, but a similar correlation was not seen in either FTLD or AD using the TDP-43 phospho-independent antibody. With the TDP-43 phospho-independent antibody, there were no significant differences in median plasma TDP-43 levels between FTLD, or AD, patients with or without TDP-43 pathology. Using TDP-43 phospho-dependent antibody, median plasma TDP-43 levels were greater in patients with, than in those without, TDP-43 pathology for FTLD patients, though not significantly so, but not for AD patients. Present assays for TDP-43 do not differentiate between FTLD, or AD, patients with or without TDP-43 pathological changes in their brains. However, the levels of phosphorylated TDP-43 in plasma do correlate with the extent of TDP-43 brain pathology in FTLD, and therefore might be a useful surrogate marker for tracking changes in TDP-43 brain pathology during the course of this disease.

Keywords Frontotemporal lobar degeneration · Alzheimer's disease · TDP-43 · ELISA · Plasma

P. G. Foulds · D. J. Hobson · K. M. Humphreys · M. Taylor · F. E. Benson · D. Allsop
Division of Biomedical and Life Sciences,
School of Health and Medicine, Lancaster University,
Lancaster LA1 4YQ, UK

Y. Davidson · D. M. A. Mann (✉)
Clinical Neurosciences Research Group,
University of Manchester, Hope Hospital,
Stott Lane, Salford M6 8HD, UK
e-mail: david.mann@manchester.ac.uk; david.mann@man.ac.uk

M. Mishra · N. Johnson · S. Weintraub · E. H. Bigio
Northwestern CNADC Neuropathology Core,
Northwestern University Feinberg School of Medicine,
710N Fairbanks Ct, Olson 2-459, Chicago, IL 60611, USA

H. Akiyama · T. Arai
Departments of Psychogeriatrics, Tokyo Institute of Psychiatry,
2-1-8 Kamikitazawa, Setagaya-ku, Tokyo 156-8585, Japan

M. Hasegawa
Department of Molecular Neuropathology,
Tokyo Institute of Psychiatry, 2-1-8 Kamikitazawa,
Setagaya-ku, Tokyo 156-8585, Japan

Introduction

Frontotemporal lobar degeneration (FTLD) describes a heterogeneous group of non-Alzheimer forms of dementia with onset of illness usually before 65 years of age arising from the degeneration of the frontal and temporal lobes. The main clinical syndrome in FTLD is frontotemporal

dementia (FTD), though related disorders of semantic dementia (SD) and progressive non-fluent aphasia (PNFA) stem from differing topographical distributions of what is considered to be a similar underlying pathology [23]. When the behavioural and personality changes of FTD are accompanied by clinical motor neurone disease (MND), the syndrome of FTD with motor neurone disease (FTD + MND) emerges [23].

About 45% cases of FTLD display insoluble tau proteins in their brains in the form of intraneuronal neurofibrillary tangles or Pick bodies [27, 30] (currently known as FTLD-tau [18]); some of these are associated with mutations in the tau (*MAPT*) gene. However, a tau-negative, ubiquitin positive (UBQ-ir) histology (FTLD-U) is the most common histological change underlying FTLD and accounts for about 55% of cases [14, 16, 20, 27, 30]. This histology is exemplified by the presence of neuronal cytoplasmic inclusions (NCI) and/or neuritic changes (DN) in cerebral cortex and the hippocampus; and in some FTLD-U cases, neuronal intranuclear inclusions (NII) of a "cat's eye" or "lentiform" appearance [15, 32] have been described, especially in cases with autosomal dominant inheritance associated with mutations in progranulin (*PGRN*) gene [4–6, 17, 26, 28]. The major protein component in most cases of FTLD-U has been identified as the TAR DNA-binding protein, TDP-43 [2, 24], and such cases are currently referred to as FTLD-TDP [18]. However, TDP-43 pathological changes are also present in the ubiquitinated NCI in patients with MND alone [2, 7, 8, 24], and in NCI in 20–25% patients with either Alzheimer's disease (AD) [1, 12, 31] or Lewy body disorders [3, 21].

In a previous study [9], we investigated whether we could detect the presence, or increased amounts, of TDP-43 in plasma of patients with FTLD and AD compared to normal control subjects. Using ELISA, we detected elevated levels of TDP-43 protein in plasma of 46% patients with clinical FTD and 22% patients with AD, compared to 8% of control subjects. Such proportions of patients with FTD and AD showing raised plasma TDP-43 levels correspond closely to those proportions known from autopsy studies to contain TDP-43 pathological changes in their brains [1, 12, 14, 16, 20, 27, 30, 31]. We considered that raised TDP-43 plasma levels might thereby reflect TDP-43 pathology within the brain and provide a biomarker that may help to distinguish those cases of FTLD-TDP from those with FTLD-tau, and those patients with AD harbouring TDP-43 pathological changes from those without such additional pathology. As a predictive test, plasma TDP-43 level could, therefore, have great practical value in directing therapeutic strategies aimed at preventing or removing tau or TDP-43 pathological changes from the brain in FTLD and AD.

However, a major limitation of the previous study was that all measurements of plasma TDP-43 level were made on living patients, and therefore, it was not possible to determine whether TDP-43 pathological changes were indeed present within the brains of those individuals displaying high plasma readings. In this present study, we have been able to examine plasma TDP-43 levels in a series of patients with autopsy confirmed FTLD and AD and thereby directly compare plasma TDP-43 levels with the presence of TDP-43 brain pathology.

Materials and methods

Patients

Brain tissues (paraffin sections) and matching plasma samples were available with Ethical Approval from 52 patients courtesy of Dr E Bigio at Northwestern CNADC Neuropathology Core, Northwestern University Feinberg School of Medicine, Chicago, USA (Table 1). Twenty-eight patients (#1–28) clinically had FTLD, or related disorder. These were classified according to recent consensus criteria [18]. Of these, 14 patients had FTLD-TDP; patients #1–6 bore progranulin gene (*PGRN*) mutations and patients #9–14 clinically had FTD or FTD + MND). Fourteen patients (#15–28) had FTLD-tau, including 1 patient (#15) with FTLD with Pick bodies, 7 patients (#16–22) with corticobasal degeneration (CBD), 4 patients (#23–26) with progressive supranuclear palsy (PSP) and 2 patients (#27 and 28) with an unclassifiable tauopathy. Twenty-four patients (#29–52) had pathologically confirmed AD (CERAD score C, Braak stage V or VI), with additional Lewy body pathology in 1 of these (#31) (Table 1). Patients with AD and FTLD fulfilled the National Institute of Neurological and Communicative Disorders and Stroke–Alzheimer's disease and Related Disorders Association (NINCDS–ADRDA) criteria for probable AD [19] and International criteria for FTLD [22], respectively.

Immunohistochemistry

Tissue sections had been cut at a thickness of 6 μm from formalin fixed, paraffin embedded blocks of frontal cortex (BA8) and temporal cortex (BA21) to include the hippocampus. Sections were immunostained for TDP-43 protein using a commercial phosphorylation-independent rabbit polyclonal anti-TDP-43 antibody (Proteintech Group Inc, Chicago, USA), as described previously [7] and for phosphorylated TDP-43 using the phospho-dependent anti-TDP-43 antibody, pS409/410 [11] at dilution of 1:1,000, using the same methodology [7].

Table 1 Clinical and pathological details of cases

Case	Sex	Onset age (years)	Age at death (years)	Duration when sampled (years)	Total duration of disease (years)	Clinical diagnosis	Pathological diagnosis	TDP pathology score (Ptech)	TDP pathology score (pS409/410)	Ptech ELISA A450 nm	pS 409/410 ELISA A450 nm
1	F	63	68	1.3	5	CBD/PPA	FTLD-TDP (type 3)	10	12	0.25	1.842
2	M	58	65	4	7	FTD	FTLD-TDP (type 3)	11	10	1.062	2.370
3	M	60	64	3	4	FTD	FTLD-TDP (type 3)	5	5	0.498	0.840
4	M	49	53	1.5	4	FTD	FTLD-TDP (type 3)	5	6	0.248	0.952
5	M	57	61	1.3	4	PPA	FTLD-TDP (type 3)	8	10	0.252	0.478
6	F	56	61	1.7	5	PPA	FTLD-TDP (type 3)	12	11	0.252	0.691
7	M	53	61	4	8	PPA	FTLD-TDP (type 3)	10	11	0.581	1.890
8	M	55	62	3	7	PPA	FTLD-TDP (type 3)	6	9	0.323	1.200
9	M	54	60	4	6	ALS + FTD	FTLD-TDP (type 2)	8	7	0.339	0.660
10	M	58	61	1.5	3	ALS + FTD	FTLD-TDP (type 2)	12	16	0.301	1.462
11	M	54	58	3.5	4	FALS + dementia	FTLD-TDP (type 2)	8	12	0.629	1.695
12	F	65	68	2.1	3	FALS + PPA	FTLD-TDP (type 2)	14	19	1.434	2.406
13	M	64	66	1	2	FTD	FTLD-TDP (type 2)	12	18	0.561	1.446
14	M	58	61	4	3	PPA + ALS	FTLD-TDP (type 2)	6	10	0.553	1.402
15	M	50	55	5	5	FTD	FTLD-tau (Picks)	0	0	0.174	0.462
16	M	67	77	4	10	CBD	FTLD-tau (CBD)	0	0	0.741	1.357
17	F	63	74	10	11	CBD	FTLD-tau (CBD)	0	0	0.195	0.509
18	M	36	44	2	8	FTD	FTLD-tau (CBD)	0	0	0.394	1.327
19	M	50	54	2.3	4	FTD	FTLD-tau (CBD)	0	0	0.505	1.660
20	M	67	78	7	11	PPA	FTLD-tau (CBD)	0	0	0.29	0.898
21	F	59	65	4	6	PPA	FTLD-tau (CBD)	0	0	0.15	0.345
22	F	58	67	2	9	PPA	FTLD-tau (CBD)	0	0	0.513	1.671
23	F	70	81	6	11	FTD	FTLD-tau (PSP)	0	0	0.665	1.823
24	M	80	87	4.6	7	MIXED	FTLD-tau (PSP)	3	6	0.271	1.228
25	F	70	84	3	14	PRAD	FTLD-tau (PSP)	9	9	0.188	0.384
26	M	81	87	5	6	PSP	FTLD-tau (PSP)	0	0	0.21	1.089
27	M	62	73	8	11	FTD	FTLD-tau (unclassifiable)	0	0	0.239	0.942
28	F	70	74	2.9	4	FTD	FTLD-tau (unclassifiable)	0	0	0.29	0.761
29	M	66	79	8	13	FTD	Mixed VaD + AD with NII	11	12	0.239	0.441
30	F	65	72	4	7	FTD	AD with NII and HS	10	9	0.171	0.318
31	F	75	84	4	9	PRAD	AD with NII + DLB	13	14	0.26	0.983
32	F	76	89	7	13	PRAD	AD with HS	3	3	1.166	2.564
33	F	74	85	5	11	PRAD	AD	9	6	0.559	1.325
34	F	59	77	7	18	PRAD	AD with HS	12	11	0.234	0.505

Table 1 continued

Case	Sex	Onset age (years)	Age at death (years)	Duration when sampled (years)	Total duration of disease (years)	Clinical diagnosis	Pathological diagnosis	TDP pathology score (Ptech)	TDP pathology score (pS409/410)	Ptech ELISA A450 nm	pS 409/410 ELISA A450 nm
35	M	70	80	6	10	PRAD	AD	1	2	0.589	1.579
36	F	71	85	5	14	PRAD	AD	14	13	0.213	0.696
37	F	70	79	4	9	PRAD	AD	0	0	0.124	0.274
38	M	54	71	10	17	PRAD	AD	0	0	0.225	0.444
39	F	73	84	1.3	11	PRAD	AD	0	0	0.187	0.450
40	F	73	81	4	8	PRAD	AD	0	0	0.225	0.833
41	M	71	77	4	6	PRAD	AD	0	0	0.398	1.244
42	M	62	69	1.3	7	PRAD	AD	0	0	1.463	2.451
43	F	76	82	3	6	PRAD	AD	0	0	0.217	0.490
44	M	64	73	5	9	PRAD	AD	0	0	0.7	1.984
45	M	59	68	5.9	9	PRAD	AD	0	0	0.335	1.103
46	M	45	50	3	5	FTD	AD	0	0	0.364	1.346
47	M	59	76	9	17	FTD	AD	0	0	0.115	0.285
48	M	53	60	1	7	FTD	AD	0	0	0.284	0.729
49	M	53	60	2	7	FTD	AD	0	0	0.18	0.758
50	M	51	72	15	21	PPA	AD	0	0	0.488	1.746
51	F	71	77	1.4	6	PPA	AD	0	0	0.225	0.841
52	F	57	64	3	7	PPA	AD	0	0	0.875	1.479

AD Alzheimer's disease, *ALS* amyotrophic lateral sclerosis, *CBD* corticobasal degeneration, *DLB* dementia with Lewy bodies, *FALS* familial motor neurone disease, *FTD* frontotemporal dementia, *FTLD* frontotemporal lobar degeneration, *HS* hippocampal sclerosis, *NII* neuronal intranuclear inclusions, *PPA* primary progressive aphasia, *PRAD* probable Alzheimer's disease, *PSP* progressive supranuclear palsy, *VaD* vascular dementia

The severity of TDP-43 pathological changes, as determined by each anti-TDP-43 antibody, was separately assessed on a 5-point scale (0 = absent, 1 = mild, 2 = moderate, 3 = severe, 4 = very severe) in layer II of frontal and temporal cortex, in dentate gyrus, areas CA4/5, CA2/3 and CA1/subiculum, entorhinal cortex and fusiform gyrus. A total severity score for each case was determined by summation of individual scores over these 8 regions giving a maximum possible score of 32 per case per antibody.

Preparation of recombinant protein

TDP-43 was expressed in *E. coli* as a His-tagged protein. The cDNA for TDP-43 was PCR amplified from EST IMAGE clone 5498250 with TDP-43-*Bam*HI sense primer 5′-AGAGGATCCATGTCTGAATATATTCGGGTAAC-3′, TDP-43-*Hin*dIII antisense primer 5′-AGAGAAAGCTT CTACATTCCCCAGCCAGAAG-3′ and subcloned into pET30a via *Bam*HI and *Hin*dIII restriction sites in-frame with the vector encoded N-terminal polyhistidine tag. His-tagged TDP-43 was overexpressed in *E. coli* Rosetta-gami 2(DE3)pLysS. Cells were lysed by sonication in 20 mM Tris–HCl pH8.0, 500 mM NaCl, 20 mM imidazole, 1 mM PMSF, 0.02%Triton X-100, 10% glycerol and soluble proteins applied to a HiTrap™ chelating column charged with nickel. Proteins were eluted from the column with a linear 20–500 mM imidazole gradient, TDP-43 containing fractions analysed by SDS–PAGE and immunoblotting, and pooled. Purity of His-TDP-43 in pooled fractions was estimated as >95%.

In order to create a standard curve for the phosphorylated TDP-43 ELISA, His-TDP-43 was coupled to the antigen peptide, CMDSKS(p)S(p)GWGM (as used for immunization to produce pS409/410–2 antibody). The conjugation involved Sulfo-KMUS (Pierce) as a heterobifunctional cross-linker to prepare the protein–peptide conjugate in a two-step reaction, as per the manufacturer's instructions.

ELISA assays

Whole blood samples (5 ml blood with EDTA acting as anti-coagulant) had been taken 1–15 years after onset of illness. From these samples, plasma was separated by routine methods, and stored in deep freeze (−80°C) until assay. Levels of TDP-43 within plasma samples were determined by ELISA, as described [9]. The ELISA plates (96-well PVC assay plates, Iwaki, Japan) were coated by overnight incubation at 4°C with 0.2 μg/ml anti-TDP monoclonal antibody (H00023435-M01, clone 2E2-D3, Abnova Corporation, Taiwan), 100 μl/well, diluted in 200 mM $NaHCO_3$ buffer, pH 9.6, containing 0.02% (w/v) sodium azide (final concentration 1:1,000). The plates were washed 3 times with PBST (PBS (0.01 M phosphate buffer, 0.0027 M potassium chloride and 0.137 M sodium chloride, pH 7.4) containing 0.05% Tween 20), and incubated with 200 μL/well of blocking buffer (PBS containing 2.5% gelatin and 0.05% Tween 20) for 2 h at 37°C. The plates were again washed 3 times with PBST, and 100 μl of the plasma samples to be tested, diluted 1:5 with PBS, were added to each of three wells. After 2 h incubation at 37°C the plates were washed 3 times with PBST, and 100 μl of the detection antibody, TDP rabbit polyclonal antibody (BC001487, Proteintech Group, Chicago) diluted to 0.2 μg/ml (1:1,000) in blocking buffer, was added per well and the plates were incubated at 37°C for 2 h. After another wash (as before), the plates were incubated with 100 μl/well of goat anti-rabbit secondary antibody coupled to horseradish peroxidase (HRP) (Sigma, UK), diluted 1:5,000 in blocking buffer, at 37°C for 1 h. The plates were then washed again with PBST, before adding 100 μl/well Sure Blue TMB Microwell Peroxidase Substrate (KPL Inc, Maryland, USA) and leaving the colour to develop for 30 min at room temperature. Finally, 100 μl/well of stop solution (0.3 M H_2SO_4) was added and absorbance values were read at 450 nm in a Victor^2 multi-function microtitre plate reader. Net absorbance was calculated by deducting the mean value obtained for a triplicate of "blank" wells containing PBS only. The recombinant His-TDP-43 protein was used to create the standard curve (Fig. 1).

This basic antibody-sandwich ELISA [9] was modified to detect only phosphorylated forms of TDP-43 protein by replacing the Proteintech phospho-independent polyclonal TDP-43 antibody as the detection antibody with the phospho-dependent polyclonal TDP-43 antibody, pS409/410–2 (Cosmobio Co Ltd, Tokyo), used at a dilution of 1:5,000: the monoclonal antibody (2E2-D3) was again chosen as the preferred capture antibody (1:1,000). The TDP-43-phosphorylated peptide/His-TDP-43 protein

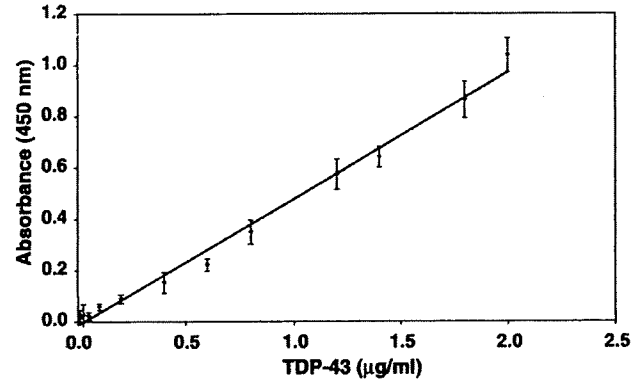

Fig. 1 Standard curve for the recombinant His-TDP-43 ELISA (data shown ± SD)

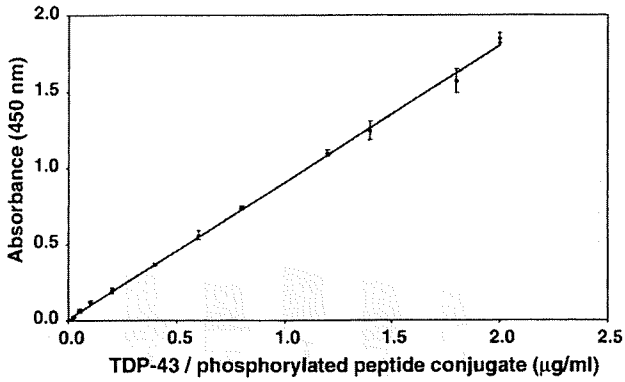

Fig. 2 Standard curve for the TDP-43, phosphorylated peptide conjugate ELISA (data shown mean ± SD)

conjugate was used in the standard curve for detection of phosphorylated forms of TDP-43 (Fig. 2).

All data were analysed using SPSS v 14.0. Because OD values from ELISA were not normally distributed (according to Kolmogorov–Smirnov test). Mann–Whitney test was employed to compare plasma TDP-43 levels between FLTD and AD groups of patients. Correlations involving ELISA data, TDP-43 pathological scores, age at onset of disease, and duration of illness when sampled, were made using Spearman rank correlation statistic.

Immunoblotting

Four plasma samples that gave relatively high absorption values (cases #12, 32, 19 and 42 detailed in Table 1) and four samples with low values (cases #5, 29, 21 and 38 detailed in Table 1), were immunodepleted of albumin and IgG (Sigma Product no. PROTIA-1KT) according to manufacturer's instructions. For SDS-PAGE, these samples were run on 12.5% polyacrylamide gels and the separated proteins were electrotransferred onto nitrocellulose membranes (0.45 μm, Invitrogen), at 25 V, 125 mA for 75 min, which were then blocked with 5% powdered, skimmed milk dissolved in PBST for 1 h. Membranes were incubated overnight with (a) phospho-independent, monoclonal anti-TDP-43 antibody (0.2 μg/ml) (H00023435-M01, clone 2E2-D3, Abnova Corporation, Taiwan), or (b) the phospho-dependent polyclonal anti-TDP-43 antibody, pS409/410-2 (Cosmobio Co Ltd, Tokyo), at a dilution of 1:5,000. The membranes were washed three times in PBST, followed by incubation with HRP-conjugated rabbit anti-mouse or goat anti-rabbit (Sigma), as appropriate, at 1:5,000 in PBST, for 1 h. The protein bands were visualised using ECL reagents (Pierce, Rockford, IL, USA) as described by the manufacturer.

Results

Immunohistochemistry

Using the phosphorylation-independent (Proteintech) TDP-43 antibody, 23/52 patients displayed TDP-43 pathological changes (Table 1). In patients #1–8, there were pathological changes in frontal and temporal cortex, and hippocampus, typical of FTLD-TDP type 3 (Fig. 3a), whereas in patients #9–14 FTLD-TDP type 2 changes were seen (Fig. 3b):

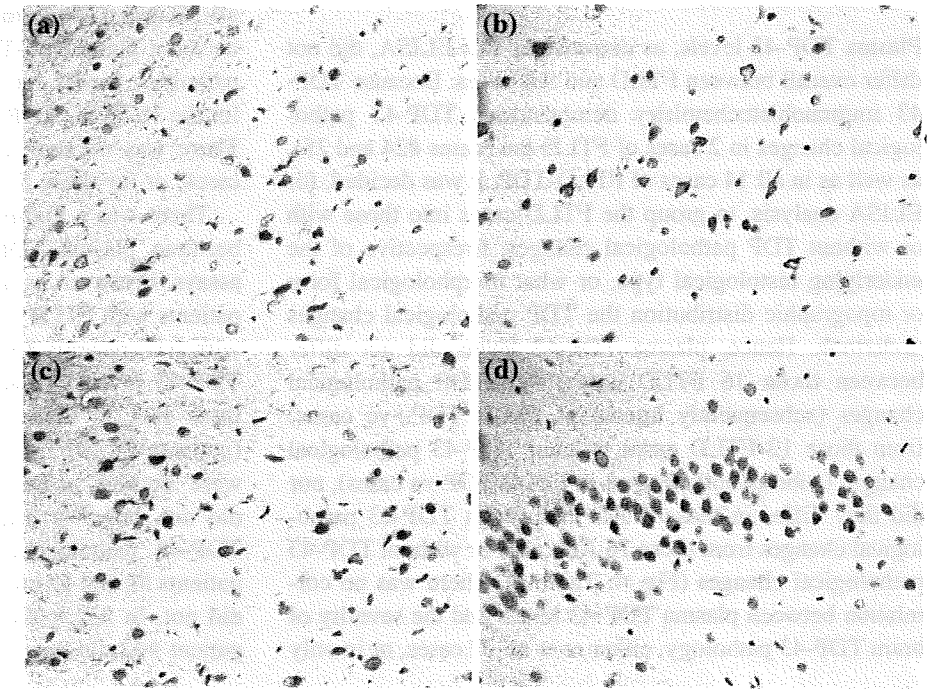

Fig. 3 Using the phosphorylation-independent (Proteintech) TDP-43 antibody, 23/52 patients displayed TDP-43 pathological changes. In FTLD-TDP patients #1–8 there were TDP-43 pathological changes in temporal cortex typical of FTLD-TDP type 3 (**a**), whereas in FTLD-MND patients #9–14 FTLD-TDP type 2 changes were seen (**b**). Two patients with PSP (patients #24 and 25) and 8 patients with AD (patients #30–37) showed TDP-43 pathological changes within the entorhinal cortex and fusiform gyrus (**c**) and dentate gyrus granule cells (**d**)

patient #15 with Pick-type histology showed no TDP-43 immunoreactive changes. Two of the 4 patients with PSP (patients #24 and 25), and 8 of the 24 patients with AD (patients #29–36), showed TDP-43 pathological changes within the entorhinal cortex and fusiform gyrus (Fig. 3c) and dentate gyrus granule cells (Fig. 3d). One patient with PSP (#25) and 6 with AD (#29–31, 33, 34 and 36) showed TDP-43 pathological changes in temporal neocortex, but only AD patients #30 and #36 showed similar changes in frontal cortex. None of the seven patients with CBD showed TDP-43 pathological changes, neither did the patient with FTLD-tau with Pick bodies nor did the two FTLD-tau patients with an unclassifiable tauopathy.

Similar results were obtained with the polyclonal phospho-dependent TDP-43 antibody, ps409/410-2, with the exception that the normal diffuse pattern of nuclear staining was not present with this antibody (Table 1). All patients and sections displaying TDP-43 pathological changes with Proteintech antibody were also immunoreactive with pS409/410 antibody, with no additional patients/sections displaying TDP-43 immunoreactivity using the latter antibody (Table 1). While in some instances, overall rating scores for TDP-43 pathology were identical using both TDP-43 antibodies, on other occasions these differed though usually only by one or two points either way (Table 1). Consequently, the pathological score using pS409/410 antibody correlated significantly with that using Proteintech antibody ($p < 0.001$).

ELISA analysis

Phospho-independent TDP-43 ELISA

Plasma TDP-43 levels, as detected by this ELISA, did not differ overall between FTLD and AD cases. Because TDP-43 immunohistochemistry demonstrated TDP-43 pathological changes in 2 cases of FTLD-tau (cases #24 and 25), as well as in all 14 cases of FTLD-TDP, it was decided, for ELISA analysis, to group the FTLD cases into those with or without TDP pathological changes, irrespective of the underlying histological type, or what morphological form or topographic distribution the TDP pathological changes undertook. Hence, plasma TDP-43 levels did not differ between those 16 FTLD cases with TDP pathological changes (subsequently known as FTLD TDP+ve cases) from those 12 FTLD cases without TDP-43 pathological changes (subsequently known as FTLD TDP-ve cases), nor did they differ in those 8 AD cases with TDP-43 pathological changes from those 16 AD cases or without TDP-43 pathological changes (Fig. 4; Table 2). There was no correlation between plasma TDP-43 levels and the severity of brain TDP-43 pathology, either over all 52 cases, or in only those 16 FTLD or 8 AD cases displaying TDP-43 pathological changes.

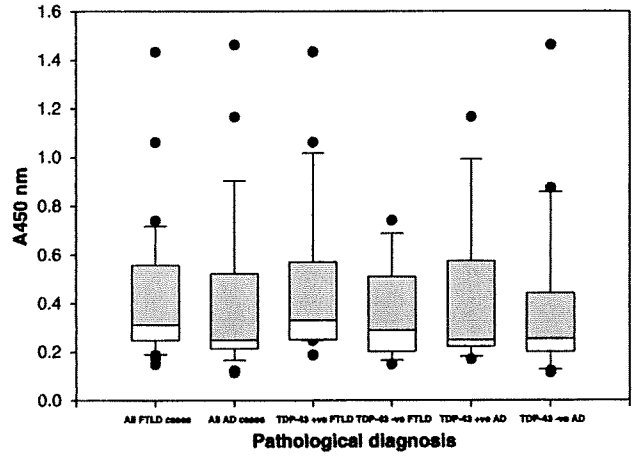

Fig. 4 Box-whisker plots for the plasma phospho-independent (Proteintech) TDP-43 ELISA results (absorbance values). The length of each *box* represents the interquartile range (75–25%) of the sample, the *solid line* drawn across the box the median, the *dashed line* the mean, and outliers are denoted by *dots*

Phosphorylated (pS) TDP-43 ELISA

Plasma pS-TDP-43 levels, as detected by this ELISA, were generally higher in FTLD TDP+ve than in FTLD TDP-ve cases (Fig. 5; Table 2) but this did not reach statistical significance. This trend was not apparent when comparing the AD TDP-43 positive and AD TDP-43 negative cases. There was no significant correlation between pS-TDP-43 levels and the severity of brain pS-TDP-43 pathology over all 52 cases. However, there was a significant correlation between plasma pS-TDP-43 levels and pS-TDP-43 histopathology scores for all 28 FTLD cases ($p = 0.037$) and for the 16 FTLD TDP+ve cases alone ($p = 0.010$) (Fig. 6). There was no such correlation for the 24 combined AD cases, or for those 8 AD cases with TDP-43 pathology.

There was a highly significant ($p < 0.0001$) correlation between plasma TDP-43 levels as determined by both assays. However, as in our previous study [8], there were 3 patients with FTLD (patients #2, 12 and 16) and 2 patients with AD (patients #32 and 42) who showed 'high' plasma TDP-43 levels in each assay (Figs. 4, 5). Two of these three FTLD 'outliers', and both of the AD 'outliers' (patients #2 and 12, and patients #32 and 42, respectively) were 'outliers' as measured by both TDP-43 ELISAs. They did not, however, match up exactly with cases showing TDP-43 pathological changes in the brain. In FTLD, patients #2 and 12 had TDP-43 pathology while patient #16 did not. In AD, patient #32 had TDP-43 pathology while patient #42 did not.

Table 2 Details of groups of patients with FTLD-TDP and FTLD-tau, and AD patients with or without TDP-43 pathological changes, at the time when blood samples were taken

	FTLD TDP+ve	FTLD TDP−ve	AD TDP+ve	AD TDP−ve
Patients (*n*)	16	12	8	16
Age at onset range (years)	49–80	36–81	59–76	45–73
Mean age at onset (years ± SD)	59.6 ± 7.5	61.1 ± 11.8	69.5 ± 5.8	61.9 ± 9.5
Age at death range (years)	53–68	44–87	72–89	50–84
Mean age at death (years ± SD)	65.0 ± 8.8	69.1 ± 12.6	65.9 ± 9.2	71.4 ± 9.3
Mean disease duration when sampled (years ± SD)	2.7 ± 1.2	4.8 ± 2.5	5.8 ± 1.5	4.6 ± 3.8
Total disease duration range (years)	2–14	4–11	7–18	5–21
Mean total disease duration (years ± SD)	5.4 ± 2.9	8.0 ± 2.9	11.9 ± 3.4	9.5 ± 4.7
Gender; Male:Female % (*n*)	79:11 (11:3)	57:43 (8:6)	25:75 (2:6)	63:37 (10:6)
Mean absorbance value (pS-independent)[a]	0.52 ± 0.35	0.34 ± .18	0.43 ± 0.34	0.40 ± 0.35
Median absorbance value (pS-independent)[a]	0.42	0.29	0.25	0.25
Mean absorbance value (pS409/410-2)[a]	1.31 ± 0.63	1.07 ± 0.50	1.03 ± 0.64	1.05 ± 0.75
Median absorbance value (pS409/410-2)[a]	1.32	1.02	0.84	0.84

Mean and median plasma TDP-43 levels as determined by phospho-independent (Proteintech) and phospho-dependent (pS409/410-2) TDP-43 antibodies are shown

AD Alzheimer's disease, *FTLD* frontotemporal Lobar Degeneration

[a] Includes 2 FTLD-tau cases positive for TDP-43 pathological changes

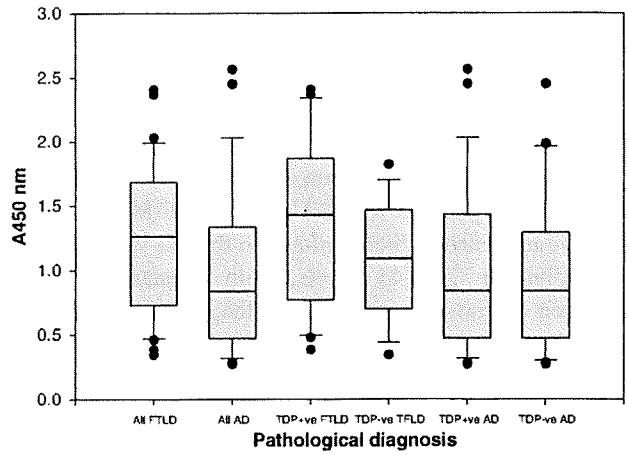

Fig. 5 Box-whisker plots for the plasma phosphodependent (pS409/410-2) TDP-43 ELISA results (absorbance values). The length of each *box* represents the interquartile range (75–25%) of the sample, the *solid line* drawn across the *box* the median, the *dashed line* the mean, and outliers are denoted by *dots*

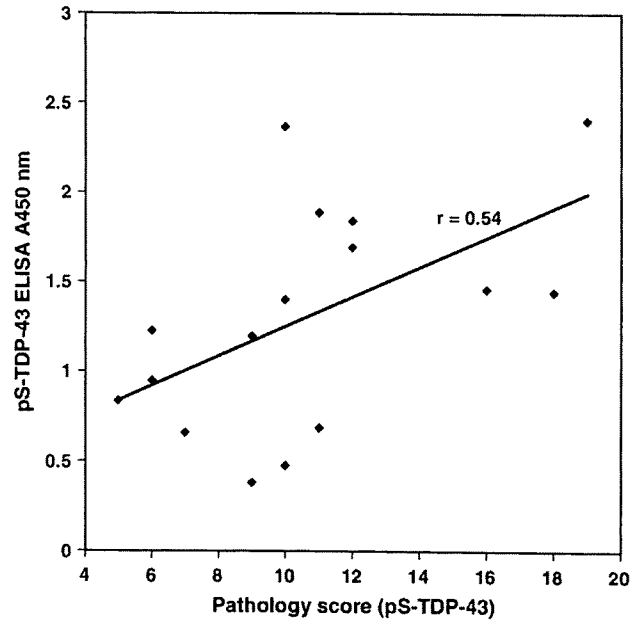

Fig. 6 Correlation ($p < 0.001$) between pS-TDP-43 ELISA and pS-TDP-43 pathological score for the 16 FTLD patients with TDP pathology

There were no significant correlations between plasma TDP-43 levels and age at onset, or duration of illness when sampled, for all 52 cases, or when these were stratified into FTLD or AD cases, using either the phospho-independent or the phospho-dependent antibody. There were also no significant correlations between TDP pathological scores and age at onset, or total duration of illness, for either FTLD or AD cases, overall or when considering only those cases that were TDP-43 positive, using either the phospho-independent or the phospho-dependent antibody.

Western blotting

Western blots were carried out in order to confirm the presence of TDP-43 and ps-TDP-43 in selected plasma samples, which were depleted of albumin and IgG (see Fig. 7). The phospho-independent, anti-TDP-43 monoclonal antibody 2E2-D3 raised against the N-terminal end of

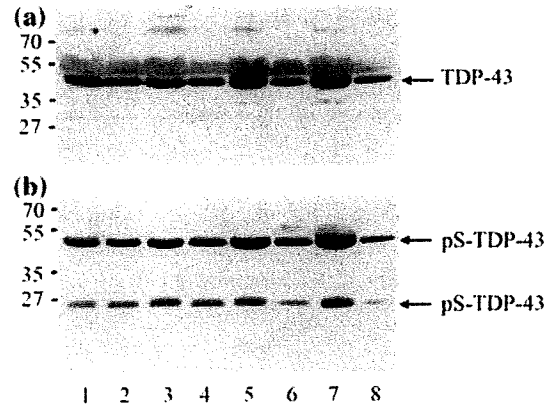

Fig. 7 Western blot analysis of plasma samples. **a** Analysis with the phospho-independent monoclonal antibody 2E2-D3 (Abnova), raised against the N-terminal end of TDP-43 (aa205–222), which recognises phosphorylated and non-phosphorylated forms of TDP-43. **b** Analysis with a polyclonal antibody pS409/410-2 (Cosmo Bio Co Ltd), raised against the C-terminal end of TDP-43 phosphorylated at Serine 409/410, which recognises full length and C-terminally truncated, phosphorylated forms of TDP-43. *Lanes 1, 3, 5* and *7* are samples from cases #12, 32, 19 and 42, respectively (detailed in Table 1), all with relatively high TDP-43 ELISA absorbance values. *Lanes 2, 4, 6* and *8* are from cases #5, 29, 21 and 38, respectively (Table 1), all with low TDP-43 ELISA values

TDP-43 (aa205–222) [33], which potentially recognises phosphorylated and non-phosphorylated forms of TDP-43, was able to detect a full-length form of TDP-43, migrating at ~45 kDa, in all samples examined (Fig. 7a). In addition, all samples also showed a fainter and more diffuse higher molecular weight band, migrating at ~55 kDa. The phospho-dependent polyclonal TDP-43 antibody, pS 409/410–2, raised against the C-terminal end of TDP-43 phosphorylated at Serine 409/410 [11], detected a full-length phosphorylated form of TDP-43, migrating at ~45 kDa, and a phosphorylated C-terminal fragment (~25 kDa) in all samples (Fig. 7b). There was also a suggestion of a higher molecular weight band (~55 kDa) in some samples (see lanes 6 and 7 in Fig. 7b). In general, the relative band densities of all of these forms of TDP-43 were greater in the plasma samples with high TDP-43 ELISA scores compared to those with low TDP-43 ELISA scores.

Discussion

In this present study, we confirm previous findings [1, 12, 31] of the presence of TDP-43 pathological changes within the medial temporal lobe of about one-third of patients with AD. However, we also noted a similar (to AD) pattern of TDP pathology in the brains of two patients with PSP (FTLD-tau). To our knowledge, this has not been reported previously. Uryu et al. [31] investigated 77 cases of PSP but did not detect TDP-43 pathology in any case. These same authors analysed 39 cases of CBD and found TDP-43 pathological changes in 6 cases. These resembled the changes of AD in two cases, but in four others, a more widespread pathology was seen which included clusters of threads resembling astrocytic plaques. In the present study, we did not observe TDP-43 pathology in any of the seven CBD cases investigated.

In our previous study [9], we presented data inferring that plasma TDP-43 levels might have utility in differentiating patients with FTLD with a TDP-43-based pathology from those who have tau-based pathology, and patients with AD who were harbouring TDP-43 pathological changes in their brains from those without such changes. However, these findings were based on living patients for whom there had been no pathological confirmation of disease diagnosis or histological characteristics. In the present study, we have investigated plasma TDP-43 levels in patients with autopsy-confirmed FTLD and AD and thereby have been able to relate plasma TDP-43 levels directly to the presence and amount of TDP-43 brain pathology.

Using the same commercial polyclonal phospho-independent TDP-43 antibody as in our previous study [9], we have shown that plasma levels of TDP-43 do not correlate with either the presence or the amount of TDP-43 brain pathology. However, TDP-43 protein can also be detected in cerebrospinal fluid (CSF) using the phospho-independent TDP-43 antibody and, on average, CSF TDP-43 levels are raised in patients with FTLD [29] and MND [13, 29] relative to control subjects, although there is wide variation in individual TDP-43 levels, with substantial overlap between diagnostic groups. Since the protein composition of CSF is more likely to reflect changes in brain pathology than that of peripheral blood plasma, further studies of TDP-43 as a CSF biomarker are warranted. It is possible that levels of CSF TDP-43 will correlate better with the formation of TDP-43 pathology in the brain and spinal cord than those in plasma.

TDP-43 proteins accumulate in phosphorylated form (pS-TDP-43) in the diseased brain [2, 24] and so it is possible that the presence or levels of pS-TDP-43 will correlate more accurately with brain pathology than the non-phosphorylated protein. With this in mind, we modified our existing ELISA protocol [9] to apply to pS-TDP-43 by using the phospho-specific antibody, pS409/410-2 [11], as detection antibody, instead of the phospho-independent antibody. In the present series of patients, the ELISA signal obtained for pS-TDP-43 in blood plasma correlated strongly with total TDP-43 levels as determined using the phospho-independent TDP-43 antibody. This suggests that our modified assay does indeed detect pS-TDP-43 and that a broadly consistent proportion of the total TDP-43 present

in plasma exists in phosphorylated form. It should be noted that we have also been able to confirm, by western blot, the presence of pS-TDP-43 proteins in human plasma. With the ELISA for pS-TDP-43, we could not, on a group basis, differentiate patients with FTLD (or AD) with TDP-43 brain pathology from those without such pathological changes. Although the median values of pS-TDP-43 were higher in FTLD TDP positive cases than in FTLD TDP-negative cases, this did not reach statistical significance. Therefore, it seems unlikely that this particular methodology can be employed for diagnostic purposes in blood plasma, although the utility of pS-TDP-43 as a diagnostic marker in CSF remains to be determined. However, our data show a positive correlation between plasma levels of pS-TDP-43 and the extent of brain pS-TDP-43 pathology in FTLD.

One potential role for any putative biomarker would be to aid the initial diagnosis of disease, and this can be divided into two separate objectives: (1) the differentiation of individuals who have acquired a particular disease from normal subjects even before any symptoms develop; and (2) the differentiation of a particular disorder from other diseases with similar symptoms after they appear. It may be the case that plasma TDP-43 levels do not fulfil either of these criteria, although our data still do not rule out the first possibility. However, once a clinical diagnosis is firmly established, then the role of the biomarker changes. One further valuable role of any biomarker is in longitudinal studies where it may be used (as a surrogate) to track the course of disease progression. This is potentially valuable in clinical trials, for example, where changes in a particular molecular marker can provide a level of objectivity, which may enable a reduction in the duration of a trial, and/or the number of patients required for significance. There is a great need for this type of biomarker in the neurodegenerative diseases, clinical trials and longitudinal studies of which are overly reliant on clinical rating scales (which often fluctuate and are at best only semi-quantitative) as a measure of disease progression. For many of these diseases, the development of biomarkers that can detect pathological progression independently of clinical symptoms would be a major advantage. Our data showing a positive correlation in FTLD overall, and in FTLD cases with TDP pathology, between plasma levels of pS-TDP-43 and the extent of pS-TDP-43 brain pathology, as detected by immunohistopathology, suggest that this protein could serve as marker of disease progression in already diagnosed patients. Given the advent of putative neuroprotective agents, there will be an increasing need for this type of biomarker in future clinical trials. This will be especially relevant if drugs are developed to inhibit the accumulation of TDP-43 in the brain.

We have shown previously [13] that, in MND, CSF TDP-43 levels are only raised in the initial stages of the disease (i.e. within 10 months of onset), falling back to control levels thereafter. In the present study, we found no correlation between plasma TDP-43 levels (either phosphorylated or non-phosphorylated) and duration after disease onset, but the minimum time from initial diagnosis to take a blood sample was 12 months and so it remains possible that testing of CSF or plasma from patients with FTLD or AD earlier than this would have been more informative.

As in our previous study [9], we observed, using both types of TDP-43 capture antibodies, a number of patients with FTLD or AD who had very high plasma TDP-43 levels. In other studies, we have detected polymorphic variations within regulatory regions of the *TARDBP* gene that influence the rate of transcription of TDP-43 mRNA. However, analysis of the patients in the present study with high plasma TDP-43 levels indicates that they were not those with a 'high expressing' TDP-43 haplotype (Pickering-Brown, personal communication). Why some patients show such high plasma TDP-43 levels remains unclear.

The data from the western blots supports the ELISA results, and reveals, for the first time, the presence of phosphorylated full-length (~45 kDa) and truncated forms of TDP-43 (~25 kDa C-terminal fragment) in plasma samples, as demonstrated with the phospho-dependent antibody. The phospho-independent antibody also detected a band at ~45 kDa, which appeared to co-migrate with the full-length form of the protein detected by the phospho-dependent antibody. This could likewise represent the phosphorylated form of the protein. The identity of the higher molecular weight band (at ~55 kDa) is unclear, but could be due to additional post-translational modification, possibly glycosylation. The development of these phospho-dependent and phospho-independent antibodies has provided powerful tools for the specific detection and discrimination of disease-associated abnormal TDP-43 species within tissues and body fluids in both immunohistochemical and biochemical studies, clarifying the histological and biochemical features of TDP pathology within the full spectrum of FTLD and MND [25], and characterising the TDP proteinopathy in other disorders such as AD, DLB and Argyrophilic grain disease [1, 3, 10, 12, 31]. They will prove to be extremely useful for the routine neuropathological diagnosis of TDP-43 proteinopathies, and for the investigation of emerging cellular and animal models of such. Further studies employing antibodies of these kinds will determine if these truncated forms are more useful as a disease marker than full-length forms of either TDP-43 or pS-TDP-43.

Acknowledgments We acknowledge support (to PGF, DA and DMAM) from The Medical Research Council through grant G0601364. EHB, MM, NJ and SW are all supported by NIH grant AG13854. KMH was supported by The George Barton Trust and MT by the Alzheimer's Research Trust.

References

1. Amador-Ortiz C, Lin W-L, Ahmed Z, Personett D, Davies P, Duara R, Graff-Radford NR, Hutton ML, Dickson DW (2007) TDP-43 immunoreactivity in hippocampal sclerosis and Alzheimer's disease. Ann Neurol 61:435–445
2. Arai T, Hasegawa M, Akiyama H, Ikeda K, Nonaka T, Mori H, Mann D, Tsuchiya K, Yoshida M, Hashizume Y, Oda T (2006) TDP-43 is a component of ubiquitin-positive tau-negative inclusions in frontotemporal lobar degeneration and amyotrophic lateral sclerosis. Biochem Biophys Res Commun 351:602–611
3. Arai T, Mackenzie IR, Hasegawa M, Nonoka T, Niizato K, Tsuchiya K, Iritani S, Onaya M, Akiyama H (2009) Phosphorylated TDP-43 in Alzheimer's disease and dementia with Lewy bodies. Acta Neuropathol 117:125–136
4. Baker M, Mackenzie IRA, Pickering-Brown SM, Gass J, Rademakers R, Lindholm C, Snowden J, Adamson J, Sadovnick AD, Rollinson S, Cannon A, Dwosh E, Neary D, Melquist S, Richardson A, Dickson D, Eriksen J, Robinson T, Zehr C, Dickey CA, Crook R, McGowan E, Mann D, Boeve B, Feldman H, Hutton M (2006) Mutations in *Progranulin* cause tau-negative frontotemporal dementia linked to chromosome 17. Nature 442:916–919
5. Boeve BF, Baker M, Dickson DW, Parisi JE, Giannini C, Jsephs KA, Hutton M, Pickering-Brown SM, Rademakers R, Tang-Wai D, Jack CR, Kantarci K, Shiung MM, Golde T, Smith GE, Geda YE, Knopman DS, Petersen RC (2006) Frontotemporal dementia and parkinsonism associated with the IVS1 + 1G → A mutation in progranulin: a clinicopathologic study. Brain 129:3103–3114
6. Cruts M, Gijselinck I, van der Zee J, Engelborghs S, Wils H, Pirici D, Rademakers R, Vandenberghe R, Dermaut B, Martin J-J, van Duijn C, Peeters K, Sciot R, Santens P, De Pooter T, Mattheijssens M, Van den Broeck M, Cujit I, Vennekens K, De Deyn PP, Kumar-Singh S, Van Broeckhoven C (2006) Null mutations in progranulin cause ubiquitin-positive frontotemporal dementia linked to chromosome 17q21. Nature 442:920–924
7. Davidson Y, Kelley T, Mackenzie IR, Pickering-Brown SM, Du Plessis D, Neary D, Snowden JS, Mann DMA (2007) Ubiquitinated pathological lesions in frontotemporal lobar degeneration contain the TAR DNA-binding protein, TDP-43. Acta Neuropathol 113:521–533
8. Dickson DW, Josephs KA, Amador-Ortiz C (2007) TDP-43 in the differential diagnosis of motor neuron disorders. Acta Neuropathol 114:71–79
9. Foulds P, McAuley E, Gibbons L, Davidson Y, Pickering-Brown SM, Neary D, Snowden JS, Allsop D, Mann DMA (2008) TDP-43 protein in plasma may index TDP-43 brain pathology in Alzheimer's disease and frontotemporal lobar degeneration. Acta Neuropathol 116:141–146
10. Fujishiro H, Uchikado H, Arai T, Hasegawa M, Akiyama H, Yokota O, Tsuchiya K, Togo T, Iseki E, Hirayasu Y (2009) Accumulation of phosphorylated TDP-43 in brains of patients with argyrophilic grain disease. Acta Neuropathol 117:151–158
11. Hasegawa M, Arai T, Nonaka T, Kametani F, Yoshida M, Hashizume Y, Beach TG, Buratti E, Baralle F, Morita M, Nakano I, Oda T, Tsuchiya K, Akiyama H (2008) Phosphorylated TDP-43 in frontotemporal lobar degeneration and amyotrophic lateral sclerosis. Ann Neurol 64:60–70
12. Hu WT, Josephs KA, Knopman DS, Boeve BF, Dickson DW, Petersen RC, Parisi JE (2008) Temporal lobar predominance of TDP-43 neuronal cytoplasmic inclusions in Alzheimer's disease. Acta Neuropathol 116:215–220
13. Kasai T, Tokuda T, Ishigami N, Sasayama H, Foulds P, Mitchell DJ, Mann DMA, Allsop D, Nakagawa M (2009) Increased TDP-43 protein in cerebrospinal fluid of patients with amyotrophic lateral sclerosis. Acta Neuropathol 117:55–62
14. Lipton AM, White CL III, Bigio EH (2004) Frontotemporal lobar degeneration with motor neuron disease-type inclusions predominates in 76 cases of frontotemporal degeneration. Acta Neuropathol 108:379–385
15. Mackenzie IRA, Feldman H (2003) The relationship between extramotor ubiquitin-immunoreactive neuronal inclusions and dementia in motor neurone disease. Acta Neuropathol 105:98–102
16. Mackenzie IRA, Baborie A, Pickering-Brown SM, Du Plessis D, Jaros E, Perry RH, Neary D, Snowden JS, Mann DMA (2006) Heterogeneity of ubiquitin pathology in frontotemporal lobar degeneration. Acta Neuropathol 112:539–549
17. Mackenzie IRA, Baker M, Pickering-Brown S, Hsiung G-YR, Lindholm C, Dwosh E, Gass J, Cannon A, Rademakers R, Hutton M, Feldman H (2006) The neuropathology of frontotemporal lobar degeneration caused by mutations in the *progranulin* gene. Brain 129:3081–3090
18. Mackenzie IRA, Neumann M, Bigio EH, Cairns NJ, Alafuzoff I, Kril J, Kovacs GG, Ghetti B, Halliday G, Holm IE, Ince PG, Kamphorst W, Revesz T, Rozemuller AJM, Kumar-Singh S, Akiyama H, Baborie A, Spina S, Dickson DW, Trojanowski JQ, Mann DMA (2009) Nomenclature for neuropathologic subtypes of frontotemporal lobar degeneration: consensus recommendations. Acta Neuropathol 117:15–18
19. Mirra SS, Heyman A, McKeel D (1991) The consortium to establish a registry for Alzheimer's disease. Part II. Standardization of the neuropathologic assessment of Alzheimer's disease. Neurology 41:479–486
20. Mott RT, Dickson DW, Trojanowski JQ, Zhukareva V, Lee VM, Forman M, Van Deerlin V, Ervin JF, Wang DS, Schmechel DE, Hulette CM (2005) Neuropathologic, biochemical, and molecular characterization of the frontotemporal dementias. J Neuropathol Exp Neurol 64:420–428
21. Nakashima-Yasuda H, Uryu K, Robinson J, Xie SX, Hurtig H, Duda JE, Arnold SE, Siderowf A, Grossman M, Leverenz JB, Woltjer R, Lopez OL, Hamilton R, Tsuang DW, Galasko D, Masliah E, Kaye J, Clark CM, Montine JB, Lee VM-Y, Trojanowski JQ (2007) Co-morbidity of TDP-43 proteinopathy in Lewy body related diseases. Acta Neuropathol 114:221–229
22. Neary D, Snowden JS, Gustafson L, Passant U, Stuss D, Black S, Freedman M, Kertesz A, Robert PH, Albert M, Boone K, Miller BL, Cummings J, Benson DF (1998) Frontotemporal lobar degeneration: a consensus on clinical diagnostic criteria. Neurology 51:1546–1554
23. Neary D, Snowden JS, Mann DMA (2005) Frontotemporal dementia. Lancet Neurol 4:771–779
24. Neumann M, Sampathu DM, Kwong LK, Truax AC, Micsenyi MC, Chou TT, Bruce J, Schuk T, Grossman M, Clark CM, McCluskey LF, Miller BL, Masliah E, Mackenzie IR, Feldman H, Feiden W, Kretzschmar H, Trojanowski JQ, M-Y LeeV (2006) Ubiquitinated TDP-43 in frontotemporal lobar degeneration and amyotrophic lateral sclerosis. Science 314:130–133
25. Neumann M, Kwong LK, Lee EB, Kremmer E, Flatley A, Xu Y, Forman MS, Troost D, Kretzschmar HA, Trojanowski JQ, Lee VM (2009) Phosphorylation of S409/410 of TDP-43 is a consistent feature in all sporadic and familial forms of TDP-43 proteinopathies. Acta Neuropathol 117(2):137–149

26. Pickering-Brown SM, Baker M, Gass J, Boeve BF, Loy CT, Brooks WS, Mackenzie IR, Martins RN, Kwok JB, Halliday GM, Kril JJ, Schofield PR, Mann DM, Hutton M (2006) Mutations in progranulin explain atypical phenotypes with variants in MAPT. Brain 129:3124–3126
27. Shi J, Shaw CL, Richardson AMT, Bailey K, Tian J, Varma AR, Neary D, Snowden JS, Mann DMA (2005) Histopathological changes underlying frontotemporal lobar degeneration with clinicopathological correlation. Acta Neuropathol 110:501–512
28. Snowden JS, Pickering-Brown SM, Mackenzie IR, Richardson AMT, Varma A, Neary D, Mann DMA (2006) Progranulin gene mutations associated with frontotemporal dementia and progressive aphasia. Brain 129:3091–3102
29. Steinacker P, Hendrich C, Sperfeld AD, Jesse S, von Arnim CAR, Lehnert S, Pabst A, Uttner I, M-Y LeeV, Trojanowski JQ, Kretzschmar HA, Ludolph A, Neumann M, Otto M (2008) TDP-43 in cerebrospinal fluid of patients with frontotemporal lobar degeneration and amyotrophic lateral sclerosis. Arch Neurol 65:1481–1487
30. Taniguchi S, McDonagh AM, Pickering-Brown SM, Umeda Y, Iwatsubo T, Hasegawa M, Mann DMA (2004) The neuropathology of frontotemporal lobar degeneration with respect to the cytological and biochemical characteristics of tau protein. Neuropathol Appl Neurobiol 30:1–18
31. Uryu K, Nakashima-Yasuda H, Forman MS, Kwong LK, Clark CM, Grossman M, Miller BL, Kretzschmar HA, Lee VM-Y, Trojanowski JQ, Neumann M (2008) Concomitant TAR-DNA-binding protein 43 pathology is present in Alzheimer disease and corticobasal degeneration but not in other tauopathies. J Neuropathol Exp Neurol 67:555–564
32. Woulfe J, Kertesz A, Munoz D (2001) Frontotemporal dementia with ubiquitinated cytoplasmic and intranuclear inclusions. Acta Neuropathol 102:94–102
33. Zhang HX, Tanji K, Mori F, Wakabayashi K (2008) Epitope mapping of 2E2-D3, a monoclonal antibody directed against human TDP-43. Neurosci Lett 434:170–174

NEUROPATHOLOGY

Neuropathology 2009 doi:10.1111/j.1440-1789.2009.01084.x

Original Article

Pseudopolyneuritic form of ALS revisited: Clinical and pathological heterogeneity

Zen Kobayashi,[1,2] Kuniaki Tsuchiya,[2,3] Tetsuaki Arai,[2] Osamu Yokota,[2,4] Sadakiyo Watabiki,[5] Hideki Ishizu,[6] Haruhiko Akiyama[2] and Hidehiro Mizusawa[1]

[1]Department of Neurology and Neurological Science, Graduate School, Tokyo Medical and Dental University, Tokyo, [2]Tokyo Institute of Psychiatry, Tokyo, [3]Department of Laboratory Medicine and Pathology, Tokyo Metropolitan Matsuzawa Hospital, Tokyo, [4]Department of Neuropsychiatry, Okayama University Graduate School of Medicine, Dentistry and Pharmaceutical Sciences, Okayama, [5]Musashino Health Development Foundation, Tokyo, and [6]Department of Laboratory Medicine, Zikei Institute of Psychiatry, Okayama, Japan

Pseudopolyneuritic form of ALS is a subtype of ALS characterized by distal weakness of the unilateral lower limb and absence of Achilles tendon reflex (ATR) at disease onset. Recognition of this form of ALS is important for clinicians because the combination of distal weakness of the lower limb and absence of ATR usually suggests peripheral neuropathy. We reviewed the clinical records of 42 autopsy-proven sporadic ALS cases and found three cases that showed onset of weakness of the unilateral lower limb with distal dominance and absence of ATR. The disease duration in the three cases was 2, 3 and 19 years, respectively. The clinical features of the patient with a course of 19 years had been restricted to lower motor neuron signs. Histopathologically, consistent findings in the three cases were severe motor neuron loss throughout the whole spinal cord, with relative preservation of the hypoglossal nucleus. Reflecting this finding, TDP-43-positive neuronal cytoplasmic inclusions in the spinal cord were sparse in two cases, and absent in a third. In the patient showing a clinical course of 19 years, mild corticospinal tract degeneration appeared to correspond to the absence of upper motor neuron signs and prolonged disease duration. In this case only, Bunina bodies were not demonstrated. In this study, we clarified the clinical and pathological heterogeneity of this form of ALS.

Key words: Achilles tendon reflex, amyotrophic lateral sclerosis, heterogeneity, pseudopolyneuritic form, TDP-43.

INTRODUCTION

Amyotrophic lateral sclerosis (ALS) is a progressive neurodegenerative disorder that affects both upper motor neurons (UMNs) and lower motor neurons (LMNs). Typically, UMN and LMN signs coexist in the affected limbs at onset, and the former manifests as hyper-reflexia.[1] One of the recent reports has described that upper-limb onset was seen in ≈ 48% of patients, and lower-limb onset in ≈ 24%.[1] At autopsy, the average loss of LMNs is ≈ 50%.[2,3]

The pseudopolyneuritic form of ALS is a subtype of ALS characterized by distal weakness of the unilateral lower limb and absence of Achilles tendon reflex (ATR) at disease onset.[4–6] The patellar and upper limbs tendon reflexes may show hyper-reflexia.[4,6] The survival time with this form has been reported to range from 30 to 69 months,[4,5,7–10] and the frequency is from 1% to 17.5%.[5,7,8,10]

Histopathologically, preferential cellular degeneration of the lumbar cord was described originally,[4] and later severe LMN loss throughout the whole spinal cord[11] and depletion of the small neurons in the intermediate zone of the anterior horn of the lumbar cord[12] were reported. However, to date information regarding the clinical and histopathological findings of this disease has been limited. The purpose of our study is to describe the clinicopathological findings of three cases of the pseudopolyneuritic form of ALS including one case that showed only LMN signs and a markedly prolonged disease duration.

MATERIALS AND METHODS

Subjects

We reviewed the clinical records of 42 autopsy-proven sporadic ALS cases including details of the symptoms at onset

Correspondence: Zen Kobayashi, MD, Tokyo Institute of Psychiatry, 2-1-8 Kamikitazawa, Setagayaku, Tokyo 156-8585, Japan. Email: zen@bg7.so-net.ne.jp

Received 20 August 2009; revised 23 October 2009 and accepted 25 October 2009.

and total clinical course, from the institutional collections at Tokyo Institute of Psychiatry in Japan. There were 19 men and 23 women. The mean age at onset was 62.3 years (range: 33–83 years). The mean disease duration of the cases without artificial respiratory support was 30.8 months (range: 2–228 months). There were 15 cases showing upper-limb onset and nine cases of lower-limb onset. In the cases showing lower-limb onset, deep tendon reflex was recorded in seven cases. Among these cases, we encountered three cases that showed onset of unilateral lower-limb weakness with distal dominance and absence of ATR. One of these cases (case 3) was previously reported.[13] For comparison, we examined specimens from 11 cases of upper-limb onset ALS and four ALS cases showing lower-limb onset with increased ATR as controls.

Conventional neuropathology and assessment of LMN loss

Brain tissue samples from all subjects were fixed post mortem with 10% formalin and embedded in parafin. Sections (10 μm thick) were prepared from the frontal, temporal, parietal, occipital, insular and cingulate cortices, hippocampus, amygdala, basal ganglia, midbrain, pons, medulla oblongata, cerebellum and spinal cord, including the cervical, thoracic, lumbar and sacral cords. These sections were stained by HE, KB and Holzer methods. The degree of LMN loss in the hypoglossal nucleus and the spinal cord was graded as mild, moderate or severe.

Immunohistochemistry and assessment of TDP-43 pathology

Antibodies used in this study are shown in Table 1. Sections from representative regions of the cerebrum, brainstem, and cervical, thoracic, lumbar and sacral cords were examined using antibodies to ubiquitin and phosphorylated TDP-43 (pS409/410).[14] In case 3, TDP-43 immunoreactivity was examined further using other anti-phosphorylated TDP-43 antibodies (pS403/404)[14] and two kinds of phosphorylation-independent antibodies (anti-TDP-43C antibodies [405–414][14] and commercially available antibodies). Hippocampal dentate granular cells of case 2 were also examined with these three anti-TDP-43 antibodies, and were further examined with anti-fused in sarcoma (FUS),[15] anti-AT8, and anti-α-synuclein antibodies. In case 3, cystatin C immunoreactivity was examined in the brainstem and spinal cord, and axons in the corticospinal tract (CST) of the spinal cord were evaluated using anti-neurofilament antibodies. The severity of TDP-43 immunoreactive pathological changes in each topographical brain area was rated as: 0 = absent; 1 = rare to mild; 2 = moderate to severe.

RESULTS

Case reports

None of the three cases had any history of ALS-like disorder in their families. Case 3 is briefly described because this case was reported previously.[13] The clinicopathological findings of the three cases are summarized in Tables 2 and 3. Distribution of TDP-43-positive inclusions is shown in Table 4.

Case 1

Clinical course. A 61-year-old Japanese man developed right dropped foot followed by left dropped foot approximately 3 months later, and presented with steppage gait. He needed a cane while walking, and consulted the Department of Neurology at a general hospital 10 months after onset. Neurological examination demonstrated muscle weakness of the distal part of the lower limbs and absence of ATR. Other tendon reflexes were within normal limits. Fasciculation was not apparent. Nerve conduction study demonstrated that motor conduction velocity was within normal limits. Needle electromyogram demonstrated neurogenic changes. Thereafter, muscle weakness of the lower limbs progressed, and he became unable to

Table 1 Antibodies used in this study

Antibody	Type	Source	Dilution
Anti-ubiquitin	Rabbit polyclonal	Dako, Glostrup, Denmark	1:2000
Phosphorylation-independent anti-TDP-43			
Anti-TDP-43	Rabbit polyclonal	ProteinTech, Chikago, IL, USA	1:1000
Anti-TDP-43C [405–414]	Rabbit polyclonal	Made by Hasegawa *et al.*[14]	1:1000
Phosphorylation-dependent anti-TDP-43			
pS409/410	Rabbit serum	Made by Hasegawa *et al.*[14]	1:1000
pS403/404	Rabbit serum	Made by Hasegawa *et al.*[14]	1:1000
Anti-FUS	Rabbit polyclonal	Sigma, St. Louis, MO, USA	1:500
Anti-tau (AT8)	Mouse monoclonal	Innogenetics, Gent, Belgium	1:100
Anti-α-synuclein (Pα#64)	Mouse monoclonal	Wako Chemical, Osaka, Japan	1:3000
Anti-cyctatin C	Rabbit polyclonal	Dako, Glostrup, Denmark	1:1000
Anti-neurofilament (SMI 31)	Mouse monoclonal	Sternberger, Lutherville, MD, USA	1:1000